Available online at www.sciencedirect.com
ScienceDirect
Trans. Nonferrous Met. Soc. China 21(2011) 215−222
Transactions of Nonferrous Metals Society of China
www.tnmsc.cn

Microstructure of cast γ-TiAl based alloy solidified from β phase region

WANG Yan[1], LIU Yong[1], YANG Guang-yu[1], LI Hui-zhong[2], TANG Bei[2]

1. State Key Laboratory for Powder Metallurgy, Central South University, Changsha 410083, China;
2. School of Materials Science and Engineering, Central South University, Changsha 410083, China

Received 13 May 2010; accepted 26 September 2010

Abstract: The microstructures and phase transformation of Ti-43Al-4Nb alloy in as-cast and heat-treated states were investigated by using optical microscopy, scanning and transmission electron microscopy as well as differential scanning calorimetry. The results show that a fine microstructure of the as-cast alloy can be obtained by solidifying through the β phase. γ grains can nucleate directly from the β phase. The coexistence of β phase and γ phase along primary α grain boundaries contributes to the decrease in the grain size of the as-cast alloy. The phase transformation sequence during solidification of the Ti-43Al-4Nb alloy is suggested as $L\rightarrow L+\beta\rightarrow\beta\rightarrow\alpha+\beta\rightarrow\alpha+\beta_r\rightarrow\alpha+\gamma+\beta_r\rightarrow$lamellae($\alpha_2+\gamma$)$+\gamma+\beta_r$. The microstructure of the alloy after heat treatment at 1 250 °C for 16 h exhibits a certain coarsening compared with that of the as-cast state. The remnant β phase can be removed by the heat treatment process due to the diffusion of Nb and the non-equilibrium state of β phase.
Key words: γ-TiAl based alloy; microstructure; phase transformation; β phase; solidification; heat treatment

1 Introduction

Intermetallic γ-TiAl based alloys are considered the most promising materials for high temperature applications in the aerospace and automotive industry[1−2]. Owing to significant mass-saving, the researches on γ-TiAl based alloys are of growing interest and much progress has already been made during the last 20 years[3−4]. The main favorable characteristic of γ-TiAl based alloys is a combination of low density, high specific stiffness and strength, good oxidation resistance and creep property up to temperatures as high as 800 °C[5−6]. However, low ductility and damage tolerance at room temperature as well as poor workability at elevated temperatures restrict their applications. For cast γ-TiAl based alloys, the deficiencies are related not only to the intrinsic brittleness of γ and α_2 phases, but also to the microstructural evolution of the ingots during solidification[7−8].

It is well known that mechanical properties of an alloy are sensitive to microstructures. Numerous studies have shown that improved tensile strength and ductility for γ-TiAl based alloys can be obtained by grain refinement[9]. Therefore, grain size is a critical issue in cast γ-TiAl based alloys since the microstructure usually consists of coarse grains originated from α solidification. The solidification path via the β phase is favorable to obtaining a fine-grained casting microstructure without significant texture and segregation[5]. The additions of ternary alloying elements such as Nb, Mo, Cr, W, Ta and V can help to enlarging the β phase region as well as stabilizing the ductile β phases with a bcc crystal structure[10−11].

Recent investigations of γ-TiAl based alloys have demonstrated that Nb is the most effective element for improving the oxidation resistance, creep strength and ductility at room temperature[12]. By stabilizing the β phase with Nb or other elements, various solid-state phase transformations and microstructural morphologies can be achieved[13−14]. In the last few years, more attention has been paid to cast γ-TiAl based alloys with a low content of Al (42% to 45%, molar fraction)[8, 15], which were reported to exhibit improved workabilities as well as good high temperature properties[16]. The dependence of aluminum and other alloying elements on the microstructures of cast γ-TiAl based alloys has been examined[8]. However, the evolution of β phase during solid-state transformations for such types of cast γ-TiAl

Foundation item: Project (14) supported by Postdoctoral Science Foundation of Central South University, China; Project (2008AA03A233) supported by the High-tech Research and Development Program of China
Corresponding author: LIU Yong; Tel: +86-731-88830406; E-mail: yonliu11@yahoo.com.cn
DOI: 10.1016/S1003-6326(11)60702-4

based alloys is not fully understood. Detailed study of the exact phase transformation process during solidification is quite essential. The present work was devoted to a systematically microstructural study of a cast Ti-Al-Nb alloy with a low Al content. The experimental findings were expected to be used as the basis of developing new as-cast γ-TiAl alloys with homogeneous and fine-grained microstructures. Particular efforts were made to investigate the thermal stability of β phase and its effect on the evolution of microstructure.

2 Experimental

The γ-TiAl alloy used in the present work had the nominal composition of Ti-43Al-4Nb (%, molar fraction). The as-cast alloy was prepared by a non-consumable electrode arc-melting furnace in argon atmosphere and cast in a water-cooled copper mould. Highly pure Ti sponge, Al and Nb-Al master alloy were used. The button was remelted several times to ensure the chemical homogeneity. The as-cast alloy was then homogenized at 1 250 °C for 16 h, and cooled in air.

Constituent phases of the alloy were determined by X-ray diffraction (XRD) analyses using Cu K_α radiation. The samples of as-cast and homogenized alloys were cut, mechanically polished and etched in a solution of 5% HF, 10% HNO_3 and 85% H_2O in volume fraction for optical metallographic observation. In order to identify the phases, the polished surfaces were examined using a Sirion200 scanning electron microscope (SEM) in backscattered electron (BSE) mode. The microscope was equipped with an energy dispersive spectroscope (EDS) and operated at 20 kV. The foils for transmission electron microscopy (TEM) were prepared by hand grinding to a thickness of 50 μm, and then thinned using a twin-jet technique in the electrolyte of 6% $HClO_4$ +35% N-butanol+59% methanol in volume fraction at 15 V and −30 °C. TEM observation was performed on a TECNAI G^2 20 microscope operated at 200 kV. Thermal analysis was performed in a NETZSCH STA 449C differential scanning calorimeter (DSC) at a heating rate of 20 °C/min.

3 Results

3.1 As-cast alloy

Fig.1 shows the optical microstructures of the as-cast Ti-43Al-4Nb alloys with different melting times. As seen from Figs.1(a−c), the as-cast microstructures of the alloys show different characteristics from the common casting microstructures, and no apparent columnar structures are observed no matter the melting times. Inhomogeneous microstructure consisting of fine grains and coarse grains with irregular lamellar structure is formed when melted three times (Fig.1(a)). With increasing the melting times to six, the as-cast microstructure is remarkably refined which exhibits relatively uniform and approximately cellular colonies (Fig.1(b)). However, the increase of the melting times from six to eight brings little change to the microstructure of the alloy, as shown in Fig.1(c). Therefore, detailed microstructural characterizations of the Ti-43Al-4Nb alloy were performed on the bars which were melted six times.

Fig.1 Optical micrographs of as-cast Ti-43Al-4Nb alloys with melting times of 3 (a), 6 (b) and 8 (c)

As shown in Fig.1(b), the as-cast microstructure of the alloy is fine-grained and the mean colony size is about 46 μm. Thus, the microstructure of the as-cast Ti-43Al-4Nb alloy is finer than that of conventional γ-TiAl alloys[17]. Fig.2 reveals the existence of ordered γ-TiAl phase with a tetragonal lattice, and ordered

α_2-Ti_3Al phase with a close-packed-hexagonal lattice. Meanwhile, a few peaks for remanent β phase have also been detected.

The presence of different phases in γ-TiAl alloy can be proved by BSE-SEM observation, since the phases with different average atomic numbers in composition are highlighted in terms of different contrast in BSE mode. Fig.3(a) shows a BSE micrograph of the as-cast Ti-43Al-4Nb alloy. Obviously, one of the major features of the as-cast microstructure is that there is a white colored network distributing inside the lamellar colonies, and along the boundaries of the colonies. The volume fraction of the white net is roughly estimated to be about 4%, and the thickness of the white imaging layers is less than 1 μm. Quantitative EDS analysis suggests that the bright phases in Fig.3(a) are enriched in Nb (about 4.6%, molar fraction). It is well known that Nb is a β-phase stabiliser[8, 18]. The presence of β phase in as-cast γ-TiAl alloys with alloying elements of β stabilizers, such as Nb, Cr, Mo and W has been reported previously[5, 8]. Thus, the white-coloured network can be attributed to the remainings of the primary β phase β_r[19]. The microsegregation of Nb to dendrite cores occurred during solidification[20], and a few primary β phases were retained after cooling to room temperature due to the enrichment in β-phase stabiliser[21−22].

In contrast, there is a black region in the BSE image of the as-cast alloy, as shown in Fig.3(a). The volume fraction of the black regions is about 12%, and the size of the black band is about 50 μm. EDS line distribution analysis was performed to identify the microsegregation in Fig.3(a). The result (Figs.3(b−e)) reveals that the interdendritic black area exhibits solidification microsegregation that is rich in Al and poor in Nb. It

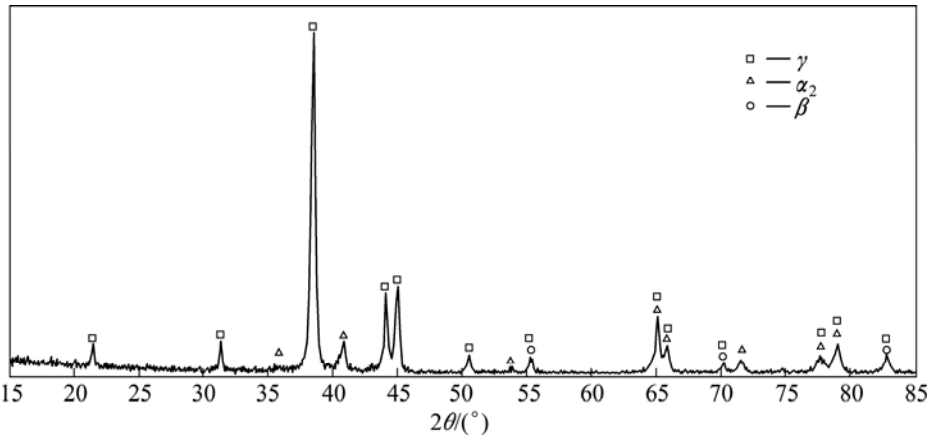

Fig.2 X-ray diffraction pattern showing phases in as-cast Ti-43Al-4Nb alloy

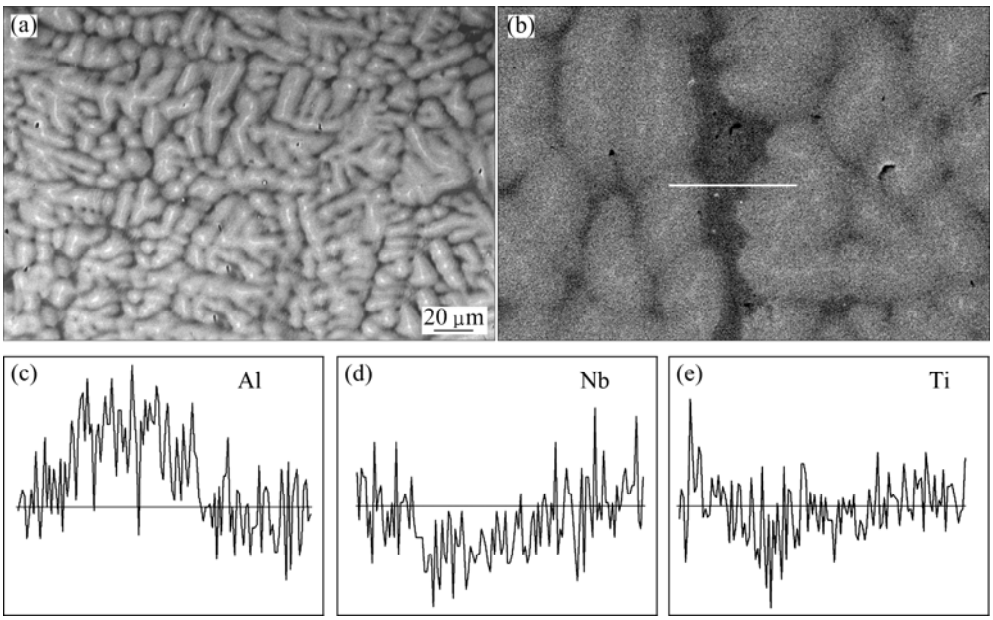

Fig.3 BSE-SEM micrograph for as-cast Ti-43Al-4Nb alloy (a) and EDS line profiles (c)−(e) showing distribution of alloying elements along line marked on micrograph (b)

may be assumed that the black regions represent the remainings of the primary solidified dendrites. The high Al concentration in the interdendritic area is ascribed to the formation of a certain amount of γ grains after cooling to the room temperature[12]. Fig.4 shows the TEM micrograph of the γ grains distributed along the boundary of the colonies and its selected area diffraction pattern.

The size of the grey region in Fig.3(a) is ranging from 15 to 60 μm. A high magnification (Fig.5(a)) provides a better view of the grey colony in Fig.3(a), which consists mainly of lamellar structures. TEM examination (Figs.5(b) and (c)) reveals that the lamellar structure is inhomogeneous and contains a large number of crystal defects. The lamellar spacing measured is in the range of 100−1 000 nm. This implies that the melting

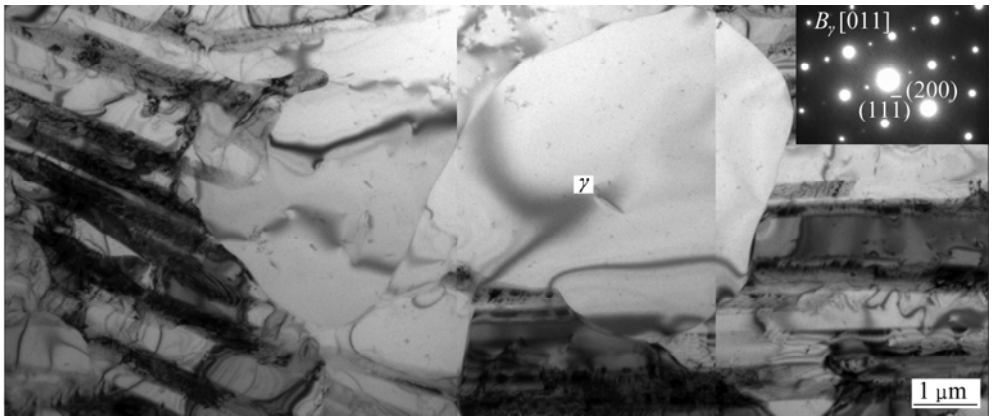

Fig.4 TEM micrograph of as-cast Ti-43Al-4Nb alloy showing phase along boundary of colonies and its diffraction pattern

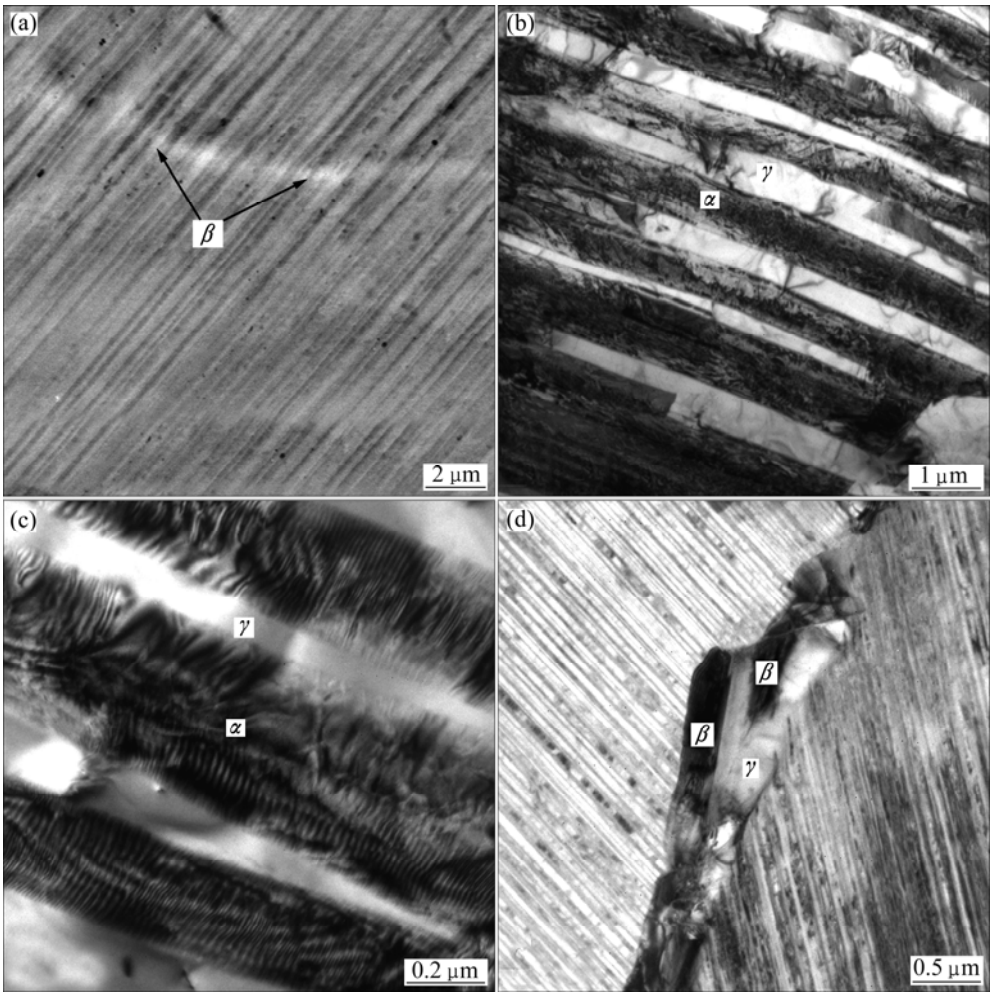

Fig.5 Micrographs of as-cast Ti-43Al-4Nb alloy showing lamellar structure inside colony (a), (b), (c) and phases along boundary of colonies (d)

method used in this investigation has a rather fast solidification rate due to the use of water-cooled copper mould. The interdendritic black regions and the colonies with lamellar structures are thus formed. It is worthwhile to note that in some areas, γ phase coupled with another phase are distributed along the boundary of the colonies (Fig.5(d)). The colonies in such regions exhibit a relatively small lamellar spacing compared with those in other regions. Those phases are determined to be β phases according to CHENG and LORETTO[23]. It is suggested that the mixture of β and γ phases might result from the cellular reaction $\beta\rightarrow\gamma$, which was also observed in other γ-TiAl alloys[23].

3.2 DSC analysis

Fig.6 shows the DSC trace for the heat-treated Ti-43Al-4Nb alloy heated up to about 1 420 °C and cooled inside the calorimeter cell. It can be seen that the DSC curves exhibit several main peaks on heating and cooling in the range of 1 200−1 420 °C, indicating the occurrence of the major solid-state reactions. On the continuous heating curve, the first signal occurred at the temperatures from 1 240 to 1 290 °C can be attributed to the transition $\alpha_2+\gamma$ to α. The transformation temperature is determined to be about 1 275 °C by tangent method, which is close to the value proposed by YIN et al[24]. The thermal effect appeared at the temperatures from 1 350 to 1 400 °C is suggested to be due to the $\gamma\rightarrow\alpha$ phase transformation. The endothermic peak at about 1 405 °C could be related to $\alpha\rightarrow\alpha+\beta$ transition. Indications for this are the appearance and shape of the peak as well as the temperature range where it appears.

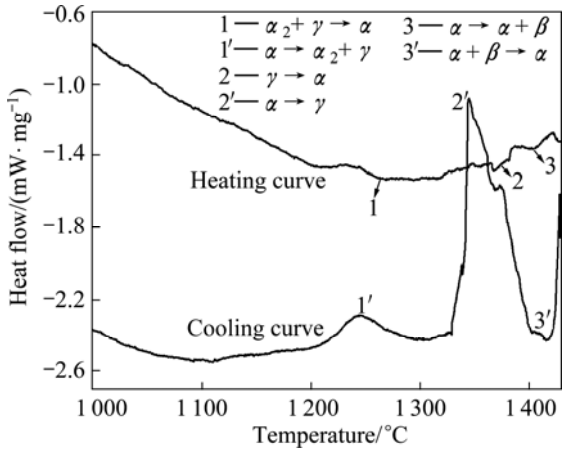

Fig.6 DSC trace of heat-treated Ti-43Al-4Nb alloy showing solid state transformations during heating and cooling

The abrupt start of solidification on cooling (Fig.6) implies that the liquid is somewhat undercooled prior to crystal nucleation. A signal with a peak at about 1 374 °C, which is indistinct on the heating curve, is detected. The exothermic peak is speculated to be linked with the $\beta\rightarrow\gamma$ transition since the reaction might occur during the cooling of the alloy. It is reported that the transformations of the α matrix in decreasing temperature for γ-TiAl based alloys take place with significant undercooling[25]. Therefore, a single broad exothermic peak appears between 1 320 and 1 200 °C, demonstrating the $\alpha\rightarrow\alpha_2+\gamma$ transition.

3.3 Heat-treated alloy

Fig.7 shows the microstructure of the as-cast Ti-43Al-4Nb alloy after being annealed at 1 250 °C for 16 h and then cooled in air. It can be noted that the microstructure of the heat-treated alloy exhibits a certain coarsening as compared with the initial as-cast condition (Fig.1(b)). The colonies become equiaxed with the mean colony size of 60−150 μm, and the mean lamellar spacing is 400−1 200 nm. The crystal defects in the lamellar structures are much less than those in the initial as-cast state, as shown in Fig.8. Obviously, diffusion is enhanced by the long exposure at 1 250 °C, which results in the coarsening $\alpha_2+\gamma$ lamellar colonies. Equiaxed or lens-shaped γ grains with a grain size of 10−30 μm

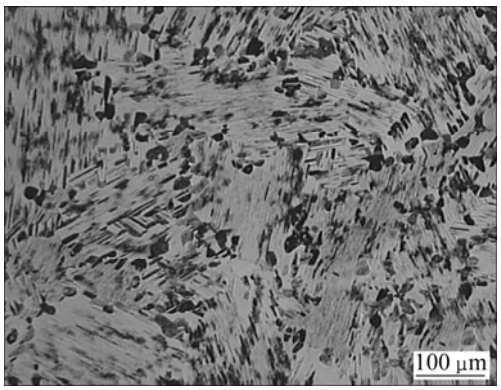

Fig.7 Optical micrograph of as-cast Ti-43Al-4Nb alloy after heat treatment at 1 250 °C for 16 h

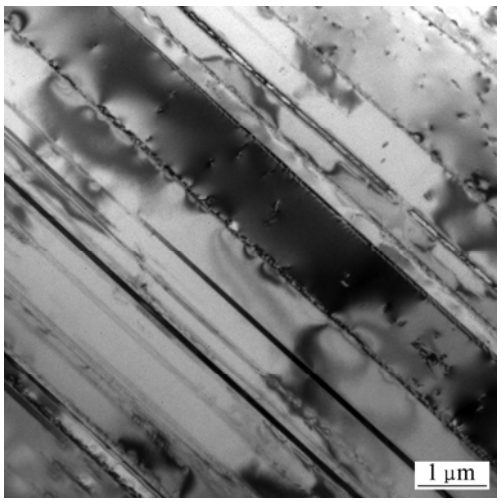

Fig.8 TEM micrograph of heat-treated Ti-43Al-4Nb alloy showing lamellar structure inside colony

are frequently observed both along the boundaries of the lamellar structures and inside the colonies (Fig.7). It should be noticed that the white network morphology of the primary β phase, which existed in the as-cast microstructure, can no longer be observed in the microstructure of the annealed sample. Thus, it suggests that the β phase in the as-cast Ti-43Al-4Nb alloy can be removed by the heat treatment process.

4 Discussion

4.1 Solidification process

The ingot has uniform fine-grained microstructure composed of lamellar colonies and γ grains as well as a few of β phases. This is mainly attributed to two reasons: 1) solidification path induced by low Al level and high Nb addition, and 2) fast solidification effect due to the melting method. The solidification path of γ-TiAl based alloys is known to be dependent on the content of Al as well as the addition of alloying elements. For the most commonly investigated alloys, solidification takes place through the α path. Since the preferential crystal growth is parallel to the c axis and there are no other orientations equivalent to the c axis in the hcp. α phase, the α crystals tend to form columnar grains along the direction of heat extraction during solidification. For the alloy investigated here, β phase is observed both inside the lamellar structures (Fig.3(a)) and along the boundary of the colonies (Fig.5(d)), which indicates that β phase is the primary solidification phase. Although the preferential growth direction of β phase during solidification is only $\langle 100\rangle$ axis, there are three equivalent directions, namely, [100], [010] and [001]. Therefore, the alloy shows a columnar character much less pronounced contrast to the case of α-solidification (Fig.3(a)).

During the following cooling, the β phase transforms to α phase, as shown in Fig.6. This transformation most likely takes place by the orientation relationship of $\{1\,\bar{1}\,0\}_\beta // (0001)_\alpha$ and $\langle 111\rangle_\beta // \langle 11\,\bar{2}\,0\rangle_\alpha$. In theory, twelve variants of α with different orientations thus form. Two different mechanisms are considered concerning the $\beta\rightarrow\alpha$ decomposition, i.e. boundary migration and secondary α lath formation[23]. Since no nucleation is required, the decomposition of β to α via interface migration can occur most readily. The lamellaes appear to have advanced into the β phase without any interruption in their morphology, as shown in Fig.5(a), which suggests that the volume fraction of the β phase decreases during cooling via the migration of the prior α/β interfaces. However, the $\beta\rightarrow\alpha$ transition via the secondary α lath formation seems to be more effective because the rather fast solidification can provide a certain undercooling that the nucleations of α inside the prior β or at α/β interfaces require. More interfacial areas for diffusion to occur are therefore obtained due to the irregular morphology of the secondary α laths.

The γ phase precipitates in a lamellar form in each α variant during the subsequent cooling. It was reported[23] that higher cooling rates can lead to the formation of Widmanstätten α plates. The large density of planar faults in these lenticular laths, which is even observed in the α_2 phase (Fig.5(c)), can presumably act as nucleation sites for γ lamellaes, leading to the occurrence of $\alpha\rightarrow\gamma$ transition. Thus, the microstructure is characterized by the presence of colonies consisted of the $\gamma+\alpha_2$ lamellar structure. A certain amount of γ grains are also observed along the boundary of the colonies, as shown in Fig.4. It is suggested from Fig.5(d) that γ grains can also nucleate directly from the β phase, compared with the transformation by discontinuous coarsening. In addition, it is possible that these γ grains originate from neighbouring γ lamellaes precipitated inside the α phases and at the α/β interfaces, which directly contact the β matrix (Fig.4). Therefore, there is no single α phase field in the investigated alloy, i.e. an $(\alpha+\gamma+\beta)$ phase field is directly below the $(\alpha+\beta)$ field. After solidification through the β path, a fine cast microstructure is developed (Fig.1(b)). The β phase and the γ phase, which co-exist along primary α grain boundaries, have also a dramatic effect on restricting the α grain growth and also perhaps the discontinuous coarsening of the lamellar spacing (Figs.5(b) and (d)).

According to the DSC results (Fig.6) and microstructural analysis above, the Ti-43Al-4Nb alloy evolves in the following phase transformation sequence during cooling: $L\rightarrow L+\beta\rightarrow\beta\rightarrow\alpha+\beta\rightarrow\alpha+\beta_r\rightarrow\alpha+\gamma+\beta_r\rightarrow$ lamellae $(\alpha_2+\gamma)+\gamma+\beta_r$.

4.2 β microsegregation and heat-treatment

The high temperature solid-state transformations lead to the formation of β-segregation for the Ti-43Al-4Nb alloy (Fig.3(a)). As the temperature drops from the β phase field to the α phase field, the $\beta\rightarrow\alpha$ transformation should take place and several α grains can nucleate in a single β grain[26]. During transformation of β/α, the Al element diffuses to α phase while the β-formation element Nb moves in the opposite direction. The EDS analysis indicates that the white network inside $\alpha_2+\gamma$ colony contains not only high Nb but also low Al (about 42.5%, molar fraction). The data imply that the Al content at the interface is also the critical requirement for the β/α transformation. The α phase can be formed as soon as Al is abounded at the interface and reaches the equilibrium concentration of α phase. With the transformation continuously proceeding, the Nb element can be abounded in the residual β phase near the

boundary of the α phases, leading to a higher Nb content at the boundary of α grains[26]. It may be assumed that, after the formation of the α phase in the interdendritic region, the α grains coarsen and grow into the former β dendrites under non-equilibrium solidification. Therefore, the remaining dendrite cores of β phase with a high Nb segregation exhibit a white network inside the assembled α phases.

However, a subsequent heat-treatment conducted at 1 250 °C for 16 h leads to a complete dissolution of the β phase, as shown in Fig.7, due to the diffusion of Nb[27] as well as the non-equilibrium state of residual β phase. Solute elements are chemically redistributed and suffciently dispersed to allow the β phase to dissolve in the disordered α phase or transform to γ phase. An increase in the colony size implies that the metastable β phase maybe also plays an important role on the limitation of the α grain growth for the Ti-Al-Nb alloy during heat treatment.

The thermodynamic stabilization of the β phase with respect to the α phase is very important in order to obtain β solidification and also provide an increased stability of the α phase against grain growth. Element Nb is selected not only due to its low diffusivity but also with the aim of providing a pronounced segregation in the β phase along the α/β interphase boundaries during the $\beta\rightarrow\alpha$ transformation. It is known that the high partition coefficient $k_{\beta/\alpha}$ would result in a kinetic stabilization of the β phase and thus hinder the grain growth when the alloy passes the α field. From the present results, elements with higher partition coefficients $k_{\beta/\alpha}$ than Nb such as W[19] should be alloyed in a small amount, so as to provide a high stability of the metastable β phase as well as the small grain size. Furthermore, suitable β phase remained after homogenizing treatment could also be favorable for the hot forging as reported by CLEMENS et al[14].

5 Conclusions

1) The microstructure of the as-cast alloy is very fine by inducing β solidification. The β phases in cast material can be eliminated by long-term heat treatment at 1 250 °C. However, a certain increase of the colony size is accompanied with the dissolution of the β phases.

2) After solidification, a small amount of remnant β phases exist either inside the lamellar colonies or along the boundaries of the colonies. The formation of γ grains in the interdendritic areas is mainly ascribed to the occurrence of $\alpha\rightarrow\gamma$ transition or the nucleation directly from the β phases.

3) The solidification paths for Ti-43Al-4Nb alloy are experimentally analyzed and determined as $L\rightarrow L+\beta\rightarrow\beta\rightarrow\alpha+\beta\rightarrow\alpha+\beta_r\rightarrow\alpha+\gamma+\beta_r\rightarrow$lamellae($\alpha_2+\gamma$)$+\gamma+\beta_r$.

References

[1] KOEPPE C, BARTELS A, SEEGER J, MECKING H. Thermomechanical treatment of two-phase intermetallic TiAl compounds [J]. Metall Trans A, 1993, 24: 1795−1806.

[2] LIU C T. Recent advances in ordered intermetallics [J]. Mater Chem Phys, 1995, 42: 77−86.

[3] ZHANG D, ARZT E, CLEMENS H. Characterization of controlled microstructures in a γ-TiAl(Cr, Mo, Si, B) alloy [J]. Intermetallics, 1999, 7: 1081−1087.

[4] KONG F T, CHEN Y Y, LI B H. Influence of yttrium on the high temperature deformability of TiAl alloys [J]. Mater Sci Eng A, 2009, 499: 53−57.

[5] CLEMENS H, BARTELS A, BYSTRZANOWSKI S, CHLADIL H, LEITNER H, DEHM G, GERLING R, SCHIMANSKY F P. Grain refinement in γ-TiAl-based alloys by solid state phase transformations [J]. Intermetallics, 2006, 14: 1380−1385.

[6] XU X J, LIN J P, WANG Y L, GAO J F, LIN Z, CHEN G L. Microstructure and tensile properties of as-cast Ti-45Al-(8-9)Nb-(W, B, Y) alloy [J]. J Alloys Compd, 2006, 414: 131−136.

[7] DIMIDUK D M, MARTIN P L, KIM Y W. Microstructure development in gamma alloy mill products by thermomechanical processing [J]. Mater Sci Eng A, 1998, 243: 66−76.

[8] IMAYEV R M, IMAYEV V M, OEHRING M, APPEL F. Alloy design concepts for refined gamma titanium aluminide based alloys [J]. Intermetallics, 2007, 15: 451−460.

[9] WANG J N, XIE K. Grain size refinement of a TiAl alloy by rapid heat treatment [J]. Scripta Mater, 2000, 43: 441−446.

[10] ZHU H L, SEO D Y, MARUYAMA K. Strengthening of lamellar TiAl alloys by precipitation bands of β_0 particles [J]. Mater Sci Eng A, 2009, 510−511: 14−19.

[11] LI B H, CHEN Y Y, HOU Z Q, KONG F T. Microstructure and mechanical properties of as-cast Ti-43Al-9V-0.3Y alloy [J]. J Alloys Compd, 2009, 473: 123−126.

[12] YANG C T, KOO C H. Improving the microstructure and high temperature properties of the Ti-40Al-16Nb alloy by the addition of a minor Sc or La-rich Misch metal [J]. Intermetallics, 2004, 12: 235−251.

[13] APPEL F, OEHRING M, WAGNER R. Novel design concepts for gamma-base titanium aluminide alloys [J]. Intermetallics, 2000, 8: 1283−1312.

[14] CLEMENS H, WALLGRAM W, KREMMER S, GÜTHER V, OTTO A, BARTELS A. Design of novel β-solidifying TiAl alloys with adjustable β/B_2-phase fraction and excellent hot-workability [J]. Adv Eng Mater, 2008, 10: 707−713.

[15] ZHANG D, DEHM G, CLEMENS H. Effect of heat-treatments and hot-isostatic pressing on phase transformation and microstructure in a β/B2 containing γ-TiAl based alloy [J]. Scripta Mater, 2000, 42: 1065−1070.

[16] CLEMENS H, CHLADIL H F, WALLGRAM W, ZICKLER G A, GERLING R, LISS K D, KREMMER S, GÜTHER V, SMARSLY W. In and ex situ investigations of the β-phase in a Nb and Mo containing γ-TiAl based alloy [J]. Intermetallics, 2008, 16: 827−833.

[17] GRANCE M, RAVIART J L, THOMAS M. Influence of microstructure on tensile and creep properties of a new castable TiAl-based alloy [J]. Metall Trans A, 2004, 35: 2087−2102.

[18] KURODA D, NIINOMI M, MORINAGA M, KATO Y, YASHIRO T. Design and mechanical properties of new β type titanium alloys for implant materials [J]. Mater Sci Eng A, 1998, 243: 244−249.

[19] KAINUMA R, FUJITA Y, MITSUI H, OHNUMA I, ISHIDA K.

Phase equilibria among α (hcp), β (bcc) and γ ($L1_0$) phases in Ti-Al base ternary alloys [J]. Intermetallics, 2000, 8: 855−867.

[20] MCCULLOUGH C, VALENCIA J J, LEVI C G, MEHRABIAN R. Peritectic solidification of Ti-Al-Ta alloys in the region of γ-TiAl [J]. Mater Sci Eng A, 1992, 156: 153−166.

[21] CHENG T T, WILLIS M R, JONES I P. Effects of major alloying additions on the microstructure and mechanical properties of γ-TiAl [J]. Intermetallics, 1999, 7: 89−99.

[22] HUANG Z W, VOICE W E, BOWEN P. Thermal stability of Ti-46Al-5Nb-1W alloy [J]. Mater Sci Eng A, 2002, 329-331: 435−445.

[23] CHENG T T, LORETTO M H. The decomposition of the beta phase in Ti-44Al-8Nb and Ti-44Al-4Nb-4Zr-0.2Si alloys [J]. Acta Mater, 1998, 46: 4801−4819.

[24] YIN W M, LUPINC V, BATTEZZATI L. Microstructure study of a γ-TiAl based alloy containing W and Si [J]. Mater Sci Eng A, 1997, 239−240: 713−721.

[25] CAGRAN C, WILTHAN B, POTTLACHER G, ROEBUCK B, WICKINS M, HARDING R A. Thermophysical properties of a Ti-44%Al-8%Nb-1%B alloy in the solid and molten states [J]. Intermetallics, 2003, 11: 1327−1334.

[26] CHEN G L, XU X J, TENG Z K, WANG Y L, LIN J P. Microsegregation in high Nb containing TiAl alloy ingots beyond laboratory scale [J]. Intermetallics, 2007, 15: 625−631.

[27] JOHNSON D R, INUI H, MUTO S, OMIYA Y, YAMANAKA T. Microstructural development during directional solidification of α-seeded TiAl alloys [J]. Acta Mater, 2006, 54: 1077−1085.

β 相区凝固的铸造 γ-TiAl 基合金的微观组织

王 岩[1], 刘 咏[1], 杨广宇[1], 李慧中[2], 唐 蓓[2]

1. 中南大学 粉末冶金国家重点实验室, 长沙 410083; 2. 中南大学 材料科学与工程学院, 长沙 410083

摘 要：采用光学显微镜(OM)、扫描电镜(SEM)、透射电镜(TEM)及差示扫描量热仪(DSC)研究 Ti-43Al-4Nb 铸态合金及其热处理态合金的显微组织以及相转变行为。结果表明：通过从 β 相区凝固的方法可以获得组织细小的铸态 Ti-43Al-4Nb 合金；凝固过程中 γ 晶能够直接从 β 相中形核，β 相与 γ 相沿初始 α 晶界共存，有效地抑制了铸态 Ti-43Al-4Nb 合金晶粒的长大；Ti-43Al-4Nb 合金在凝固过程中的相转变顺序为 $L\rightarrow L+\beta\rightarrow\beta\rightarrow\alpha+\beta\rightarrow\alpha+\beta_r\rightarrow\alpha+\gamma+\beta_r\rightarrow(\alpha_2+\gamma)$片层$+\gamma+\beta_r$；经 1 250 °C、16 h 热处理后，Ti-43Al-4Nb 合金的显微组织与铸态组织相比有一定程度的粗化；由于 Nb 元素的充分扩散以及 β 相的非平衡状态，经过上述热处理过程后残余 β 相能够被完全消除。

关键词：γ-TiAl 基合金; 显微组织; 相转变; β 相; 凝固; 热处理

(Edited by LI Xiang-qun)